iTRAQ-coupled 2D LC/MS-MS analysis of CXCR7-transfected papillary thyroid carcinoma cells: A new insight into CXCR7 regulation of papillary thyroid carcinoma progression and identification of potential biomarkers

HENGWEI ZHANG[1], LEI YANG[2], ZHANGYI LIU[1], CHENXI LIU[1], XUYONG TENG[1], LEI ZHANG[1], BO YIN[3] and ZHEN LIU[1]

[1]Department of General Surgery, Shengjing Hospital of China Medical University, Shenyang, Liaoning 110004; [2]Department of General Surgery, The First Affiliated Hospital, China Medical University, Shenyang, Liaoning 110001; [3]Department of Urology, Shengjing Hospital of China Medical University, Shenyang, Liaoning 110004, P.R. China

Received November 10, 2015; Accepted April 21, 2017

DOI: 10.3892/ol.2017.6574

Abstract. Previous studies have demonstrated that C-X-C chemokine receptor type 7 (CXCR7) regulates papillary thyroid carcinoma (PTC) growth and metastasis; however, the molecular mechanisms underlying this regulation remain unclear. In the present study, the protein expression profiles of the PTC cell line GLAG-66 and GLAG-66 cells stably transfected with CXCR7 cDNA were analyzed and compared using isobaric tag for relative and absolute quantification-coupled two-dimensional liquid chromatography-tandem mass spectrometry. In total, 2,983 proteins were quantified and 130 proteins were identified to be differentially expressed, of which 87 were significantly upregulated and 43 were significantly downregulated. Gene Ontology enrichment analysis revealed that the differentially expressed proteins were primarily enriched in a number of biological processes, including metabolism-related processes, cellular component organization, transport, cellular development process and the immune response. The differentially expressed proteins identified included fibronectin 1, basigin, periplakin and serpin family B member 5, all of which are associated with cellular junctions and cancer progression. In addition, transgelin-2 and AHNAK nucleoprotein 2 were identified as potential novel biomarkers for the prognosis and treatment of PTC.

Correspondence to: Professor Bo Yin, Department of Urology, Shengjing Hospital of China Medical University, 36 Sanhao Street, Shenyang, Liaoning 110004, P.R. China
E-mail: yinb@sj-hospital.org

Professor Zhen Liu, Department of General Surgery, Shengjing Hospital of China Medical University, 36 Sanhao Street, Shenyang, Liaoning 110004, P.R. China
E-mail: liuzhen1973@aliyun.com

Key words: papillary thyroid carcinoma, C-X-C chemokine receptor type 7, isobaric tag for relative and absolute quantification-coupled two-dimensional liquid chromatography-tandem mass spectrometry analysis

Introduction

Thyroid carcinoma is the most common endocrine neoplasm, of which papillary thyroid carcinoma (PTC) is the most common pathological type, accounting for 80% of thyroid carcinomas (1,2). Cervical lymph node metastasis is a typical clinical feature of PTC and is a risk factor for increased recurrence rates and decreased survival rates (3,4). Therefore, the identification of potential biomarkers that may be used to assess the prognosis and treatment of PTC is required.

Chemokines and their receptors serve critical roles in the development and progression of tumors (5), particularly in promoting cell migration (6). Previous studies have demonstrated that C-X-C chemokine receptor type 7 (CXCR7) expression serves a role in tumor cell proliferation, angiogenesis, invasion and metastasis (7-10). A previous study from our laboratory demonstrated that CXCR7 was overexpressed in PTC tissue compared with peritumoral non-malignant tissue and benign thyroid lesion tissue, and the expression of CXCR7 was positively associated with cervical lymph node metastasis (11). Furthermore, knockdown of CXCR7 in PTC cells has been demonstrated to suppress cell proliferation and invasion, and promote apoptosis (12), which suggests that CXCR7 is involved in the regulation of PTC progression.

In a previous study, to reveal the molecular mechanisms underlying CXCR7-mediated regulation of PTC progression, a gene microarray analysis was performed to detect changes in gene expression between PTC cells and PTC cells transfected with CXCR7. The results demonstrated that CXCR7 promotes the growth and metastasis of PTC via the activation of the phosphoinositide 3-kinase (PI3K)/RAC-α serine/threonine-protein kinase (AKT)/nuclear factor-κB (NF-κB) signaling pathway and regulation of the expression of effector molecules, including fibronectin 1 (FN1), collagen-α-1(I) chain precursor,

collagen-α-1(IV) chain precursor, platelet-derived growth factor receptor β, stromelysin-3 precursor and membrane type 1 matrix metalloproteinase 1 (13).

The aim of the present study was to investigate the molecular mechanisms underlying CXCR7-regulated PTC progression and to identify novel biomarkers for PTC. To achieve this, isobaric tag for relative and absolute quantification (iTRAQ)-coupled two-dimensional liquid chromatography-tandem mass spectrometry (2D LC-MS/MS) was used to detect alterations in protein expression profiles between GLAG-66 and GLAG-66 cells transfected with CXCR7 cDNA (GLAG-66-CXCR7).

Materials and methods

Cell lines and culture conditions. The human PTC cell line GLAG-66 was purchased from the European Collection of Authenticated Cell Cultures (Salisbury, UK). A GLAG-66-CXCR7 cell line (GLAG-66 cells stably transfected with CXCR7 cDNA) was constructed in a previous study (10). Cell lines were cultured in Dulbecco's modified Eagle's medium: Ham's F12: MCDB105 supplemented with 10% fetal bovine serum (FBS) and 2 mmol/l glutamine (all from Sigma-Aldrich; Merck KGaA, Darmstadt, Germany), as described previously (14), at 37˚C with 5% CO_2.

Cell lysis, protein isolation, digestion and labeling with iTRAQ reagents. Experimental group cells (GLAG-66-CXCR7-1) and the control cells (GLAG-66-1) were collected and lysed with 300 μl cell radioimmunoprecipitation lysis solution with 1% protease inhibitor (both from Beyotime Institute of Biotechnology, Haimen, China) containing 8 M urea on ice with regular vortex-mixing for 30 min. The mixture was centrifuged at 15,000 x g for 1 h at 4˚C, the supernatant was removed and a Bradford Protein Assay reagent kit (Beyotime Institute of Biotechnology) was used to quantify the total protein. A 100 μg amount of each sample was precipitated with 4X sample volume of ice-cold acetone at -20˚C for ~3 h and centrifuged at 20,000 x g for 20 min at 4˚C, carefully decanting the supernatant. Subsequently, according to the iTRAQ protocol (Applied Biosystems; Thermo Fisher Scientific, Inc., Waltham, MA, USA), as described previously (15), the protein was dissolved and denatured, and cysteine residues were blocked. Each sample was then digested with 20 μl 0.25 μg/μl sequencing grade modified trypsin solution (Promega Corporation, Madison, WI, USA) at 37˚C for 12 h and labeled with the iTRAQ tags as follows: GLAG-66-CXCR7-1, iTRAQ 114 (114); GLAG-66-CXCR7-2, iTRAQ 115 (115); GLAG-66-1, iTRAQ 116 (116); and GLAG-66-2, iTRAQ 117 (117), then incubated at room temperature for 2 h and vacuum-dried. The experiments were repeated in duplicate.

iTRAQ-coupled 2D LC-MS/MS analysis. The proteome analysis was performed by the Beijing Proteome Research Center (Beijing, China). In brief, the mixed iTRAQ labeled sample was centrifuged at 13,800 x g for 10 min and the supernatant was eluted with 50% buffer B (98% acetonitrile, 1.9% H_2O and 0.1% formic acid) at a flow rate of 0.4 ml/min for 10 min, then with 100% buffer A (1.9% acetonitrile, 98% H_2O and 0.1% formic acid) at a flow rate of 0.4 ml/min for 15 min. The mixture was then separated on a C_{18} reverse-phase pre-column (5 μm, 150 Å, 4.6x250 mm; Agela Technologies, Wilmington, DE, USA) at a flow rate of 1 ml/min. The gradient elution started at 5% buffer B and was followed by an increase from 5 to 18% in buffer B for 17 min, from 18 to 32% buffer B for 26 min, 32 to 95% buffer B for 28 min and finally to 5% buffer B for 40 min. The fractions were collected at 1-min intervals. All 40 fractions were centrifuge-dried at 12,000 x g at 4˚C for 15 min. Finally, the sample was resuspended with buffer A, centrifuged at 12,000 x g for 10 min. MS/MS analysis data was acquired from *m/z* 350 to 1250 with ≤2 precursors selected for MS/MS from *m/z* 100 to 1500 using dynamic exclusion.

Western blot analysis. Protein was extracted from cells according to the aforementioned protein extraction protocol. Protein concentrations were determined using a Bradford Protein Assay reagent kit (Beyotime Institute of Biotechnology, Nanjing, China). Total protein samples (80 μg/lane) were separated using 10% SDS-PAGE and then transferred onto polyvinylidene fluoride membranes. Following blocking with 5% non-fat dry milk for 2 h, membranes were incubated with primary antibodies overnight at 4˚C. The membranes were incubated for 2 h at room temperature with secondary antibodies. Antibodies used in the present study included the following: rabbit polyclonal anti-FN1 (dilution, 1:400; cat no. BA1771), anti-basigin precursor (BSG; dilution, 1:500; cat no. PB0239) (both from Boster Biological Technology, Pleasanton, CA, USA), rabbit polyclonal anti-periplakin (PPL; dilution, 1:5,000; cat no. 72422), mouse polyclonal anti-AHNAK nucleoprotein 2 (AHNAK2; dilution, 1:1,000; cat no. ab70053) (both from Abcam, Cambridge, UK), rabbit polyclonal anti-transgelin-2 (TAGLN2; dilution, 1:1,000; cat no. 10234-2-AP), β-catenin (dilution, 1:5,000; cat no. 51067-2-AP), anti-serpin family B member 5 (SERPINB5; dilution, 1:5,000; cat no. 11,722-1-AP) and GAPDH (dilution, 1:10,000; cat no. 10,494-1-AP) (all from ProteinTech Group, Inc., Chicago, IL, USA), and goat anti-rabbit and goat anti-mouse immunoglobulin G (dilution, 1:2,000; cat nos. TA130015 and TA130001; OriGene Technologies, Inc., Beijing, China) as secondary antibodies. Binding was detected using BeyoECL Plus kit (Beyotime Institute of Biotechnology). The ratio between the integrated optical density of interest proteins and GAPDH of the same sample was calculated as the relative content of protein detected using ImageJ 1.48v (National Institutes of Health, Bethesda, MD, USA). All experiments were performed three times.

Gene Ontology (GO) analysis. To analyze the functions of the differentially expressed proteins, GO analysis was performed. The GOfact (http://lidong.ncpsb.org/gofact/cgi/gofact2009.cgi) strategy was used to evaluate the biological processes, molecular functions and cell components associated with each differentially expressed protein.

Statistical analysis. For iTRAQ, raw data processing, protein identification, protein quantification, and statistical analyses were performed with ProteinPilot™ Software Beta (version 4.2; SCIEX, Framingham, MA, USA). Protein quantification ratios were $\log_{10}$-transformed. Unpaired Student's t-test was applied to analyze differences in GO and western blot analysis

Table I. Top upregulated and downregulated proteins from analysis of isobaric tag for relative and absolute quantification-coupled two-dimensional liquid chromatography-tandem mass spectrometry data.

Genes	Description	Log ratio (O/N)[a]	P-value[b] (differentially expressed)	Regulation
FN1	Fibronectin 1	1.442	$1.02x10^{-4}$	Up
ALB	Serum albumin preproprotein	1.414	$6.55x10^{-3}$	Up
TAGLN2	Transgelin-2	1.398	$2.02x10^{-5}$	Up
XRCC5	X-ray repair cross-complementing protein 5	1.372	$4.40x10^{-9}$	Up
HIST3H2BB	Histone H2B type 3-B	1.368	$3.38x10^{-2}$	Up
BSG	Basigin isoform 2	1.360	$1.16x10^{-2}$	Up
CAST	Calpastatin isoform f	1.358	$2.25x10^{-2}$	Up
PPL	Periplakin	1.342	$2.64x10^{-9}$	Up
TG	Thyroglobulin precursor	1.278	$1.30x10^{-10}$	Up
AHNAK2	AHNAK nucleoprotein 2	1.272	$4.02x10^{-3}$	Up
SARDH	Sarcosine dehydrogenase, mitochondrial precursor	-0.824	$7.31x10^{-3}$	Down
ABCB1	Multidrug resistance protein 1	-0.708	$2.92x10^{-4}$	Down
ENO3	β-enolase isoform 1	-0.696	$6.54x10^{-4}$	Down
RPL10	60S ribosomal protein L10	-0.668	$8.42x10^{-4}$	Down
CTNNB1	Catenin β-1	-0.654	$1.50x10^{-4}$	Down
SERPINB5	Serpin family B member 5	-0.632	$1.41x10^{-2}$	Down
SDHA	Succinate dehydrogenase	-0.614	$1.16x10^{-2}$	Down
PPM1G	Protein phosphatase 1G	-0.614	$3.54x10^{-3}$	Down
ALDH2	Aldehyde dehydrogenase, mitochondrial isoform 1 precursor	-0.612	$4.66x10^{-4}$	Down
UBE2L3	Ubiquitin-conjugating enzyme E2 L3 isoform 4	-0.612	$7.93x10^{-3}$	Down

[a]Log ratio (O/N) is the logarithm of fluorescence intensity ratio of O and N, where O is the experimental group (GLAG-66 cells transfected with CXCR7) and N is the control group (GLAG-66 cells). Log ratios ≥0.3 and P<0.05 represent differentially expression proteins. [b]P-value indicates the significance of log ratio (O/N).

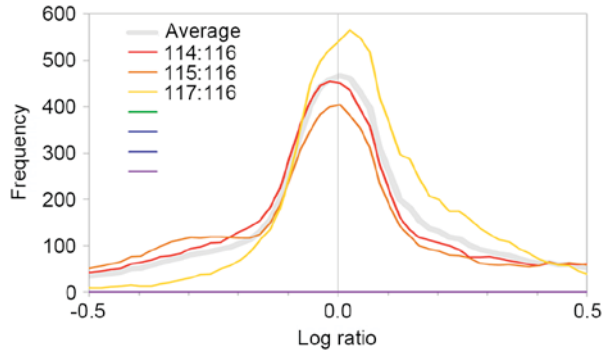

Figure 1. Distribution of protein quantification ratios. Distribution of 114:116 and 115:116 exhibit a high similarity, whereas 117:116 is markedly different.

data using SPSS software (version 19.0; IBM Corp., Armonk, NY, USA). All data are expressed as the mean ± standard deviation. P<0.05 was considered to indicate a statistically significant difference.

Results

Protein quantification ratio distribution trend. Quantification ratios among the protein sample groups (114:116, 115:116 and 117:116) were log_{10}-transformed in order to create a distribution diagram of protein quantification ratios (Fig. 1). The log_{10}-transformed protein quantification ratios were represented by fold change, and log ratios ≥0.3 or ≤-0.3 represented a 2-fold change in expression.

Proteome analysis by iTRAQ-coupled 2D LC-MS/MS. A total of 24,673 peptides and 2983 proteins were identified by iTRAQ-coupled 2D LC-MS/MS (false discovery rate, <1%). Standard selection criteria to identify differentially expressed proteins were as follows: log ratio of ≥0.3 and P<0.05 for 114:116 and 115:116 ratios (meaning the protein was differentially expressed proteins between GLAG-66 and GLAG-66-CXCR7 cells; log ratios ≥0.3 represented upregulated proteins and log ratios ≤-0.3 represented downregulated proteins) in addition to a log ratio <0.3 and P≥0.05 for 117:116 (meaning the expression was not significantly altered between the control samples). A total of 130 proteins were revealed to be differentially expressed. Among them, 87 and 43 proteins were significantly upregulated and downregulated, respectively. The top 10 differentially expressed proteins are listed in Table I. Proteins selected for further verification and analysis included FN1, TAGLN2, BSG, PPL, AHNAK2, β-catenin and SERPINB5, as they were significantly differentially expressed, and are associated with tumor development (16-22).

Table II. Top gene ontology enrichment analysis terms.

Function category	k/K[a] (%)	P-value[b]
Biological process		
Primary metabolic process	43.30	4.20×10^{-4}
Cellular metabolic process	40.00	1.90×10^{-4}
Macromolecule metabolic process	34.80	2.00×10^{-5}
Cellular component organization	32.60	3.70×10^{-33}
Transport	21.10	1.60×10^{-2}
Cellular developmental process	20.00	1.40×10^{-22}
Anatomical structure morphogenesis	17.80	5.20×10^{-32}
Response to stress	17.40	2.00×10^{-9}
Catabolic process	14.30	4.20×10^{-3}
Immune response	13.70	2.50×10^{-25}
Molecular function		
Protein binding	46.20	1.40×10^{-31}
Nucleotide binding	26.70	3.00×10^{-9}
Ion binding	18.90	4.90×10^{-3}
Transferase activity	7.10	8.50×10^{-8}
Transporter activity	5.00	2.00×10^{-3}
Signal transducer activity	4.40	3.00×10^{-10}
Lipid binding	4.40	8.70×10^{-3}
Carbohydrate binding	3.70	2.20×10^{-4}
Transmembrane transporter activity	3.70	3.20×10^{-3}
Transcription regulator activity	1.50	2.50×10^{-11}
Cell component		
Intracellular part	80.40	8.00×10^{-27}
Intracellular organelle	58.90	2.30×10^{-10}
Membrane-bounded organelle	54.50	2.80×10^{-11}
Membrane	48.40	4.00×10^{-13}
Intracellular organelle part	41.90	2.10×10^{-15}
Protein complex	34.20	1.30×10^{-38}
Non-membrane-bounded organelle	20.90	1.30×10^{-5}
Cell projection	14.00	4.80×10^{-31}
Vesicle	8.50	3.90×10^{-15}
Intracellular	8.10	9.90×10^{-7}

[a]k/K is the ratio of k and K, where k is the number of differentially expressed proteins in the corresponding Function category of the Gene Ontology analysis, and K is the total number of differentially expressed proteins within the whole analysis; [b]p-value indicates the degree of enrichment within the Function category. Smaller P-values indicate more significant category enrichment (compared with the overall distribution).

Gene Ontology (GO) enrichment analysis. To analyze function distribution in the differentially expressed proteins, a GO enrichment analysis was performed. GO enrichment analysis revealed that the differentially expressed proteins were primarily enriched in a number of biological processes, including metabolism-associated processes, cellular component organization, transport, cellular development processes and immune response. In molecular function, the differentially expressed proteins were significantly enriched in protein binding, nucleotide binding and ion binding. In cell component organization, the majority of the identified proteins were involved in intracellular part, as illustrated in Table II.

Table III. Protein expression of differentially expression proteins in GLAG-66 cells and GLAG-66-CXCR7 cells.

Gene	Protein expression (mean ± standard deviation)	P-value
FN1		<0.001
GLAG-66	0.824±0.031	
GLAG-66-CXCR7	0.274±0.022	
BSG		0.024
GLAG-66	0.648±0.016	
GLAG-66-CXCR7	0.305±0.018	
PPL		<0.001
GLAG-66	0.489±0.056	
GLAG-66-CXCR7	0.312±0.017	
TAGLN2		0.002
GLAG-66	0.534±0.050	
GLAG-66-CXCR7	0.248±0.050	
AHNAK2		0.001
GLAG-66	0.614±0.045	
GLAG-66-CXCR7	0.291±0.010	
β-catenin		<0.001
GLAG-66	0.349±0.018	
GLAG-66-CXCR7	0.756±0.015	
SERPINB5		<0.001
GLAG-66	0.333±0.015	
GLAG-66-CXCR7	0.798±0.003	

CXCR7, C-X-C chemokine receptor type 7; FN1, fibronectin 1; BSG, basigin; PPL, periplakin; TAGLN2, transgelin-2; AHNAK2, AHNAK nucleoprotein 2; SERPINB5, serpin family B member 5.

Verification of differentially expressed proteins. To confirm the differences in protein profile expression between control GLAG-66 and GLAG-66-CXCR7 cells, the upregulated proteins FN1, BSG, PPL, TAGLN2 and AHNAK2, and the downregulated proteins β-catenin and SERPINB5, were selected for further verification. Western blot analysis demonstrated that protein expression levels of FN1, BSG, PPL, TAGLN2 and AHNAK2 were significantly elevated in GLAG-66-CXCR7 cells compared with GLAG-66 cells, whereas β-catenin and SERPINB5 were significantly downregulated ($P<0.05$; Fig. 2 and Table III), which was consistent with the proteome data.

Discussion

Previous studies from our group demonstrated that overexpression of CXCR7 in PTC tissue was positively associated with lymph node metastasis, whereas knockdown of CXCR7 in PTC cells suppressed cell proliferation and invasion, and promoted apoptosis (11,12). Furthermore, gene expression profile analysis demonstrated that CXCR7 activates the PI3K/AKT/NF-κB

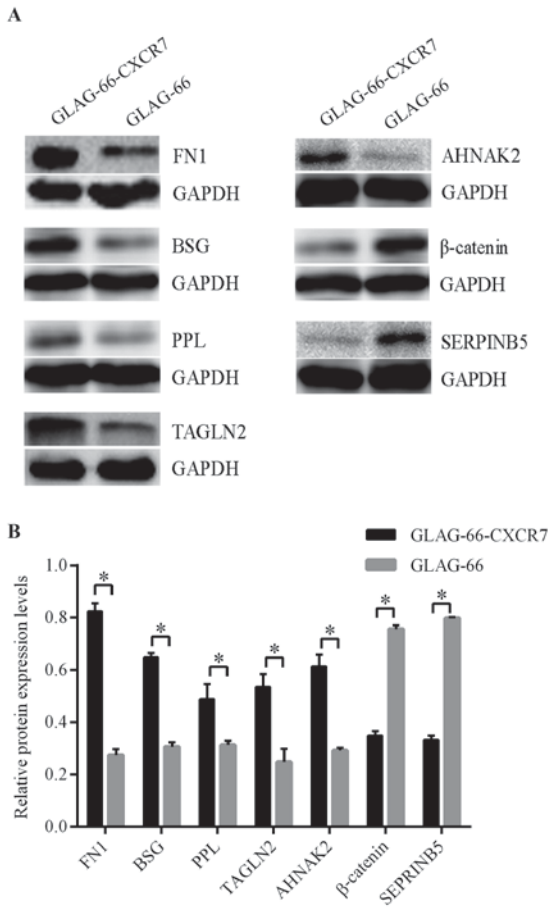

Figure 2. Protein expression of differentially expression proteins in GLAG-66 and GLAG-66-CXCR7 cells. (A) Western blot analyses of differentially expression proteins. GAPDH protein was used as a control. (B) Quantification of relative protein levels of differentially expression proteins. *P<0.05. FN1, fibronectin 1; BSG, basigin; PPL, periplakin; TAGLN2, transgelin-2; AHNAK2, AHNAK nucleoprotein 2; SERPINB5, serpin family B member 5.

signaling pathway and regulates the expression of effector molecules, thereby regulating PTC progression (13). To further evaluate the molecular mechanisms underlying CXCR7-regulated PTC growth and metastasis, in addition to screening potential biomarkers, iTRAQ-coupled 2D LC-MS/MS was performed to detect protein expression profile alterations between the GLAG-66 and GLAG-66-CXCR7 cell lines. A total of 130 differentially expressed proteins were identified, among which 87 were upregulated and 43 were downregulated.

In the present study, GO enrichment analysis revealed that the differentially expressed proteins were primarily involved in primary metabolic processes, cellular metabolic processes, macromolecule metabolic processes, cellular component organization, transport, cellular developmental processes, biological processes and protein-binding molecular function. The GO enrichment analysis of cell component revealed that the differentially expressed proteins were primarily intracellular. Certain differentially expressed proteins possessed known functions, including FN1, BSG, PPL, SERPINB5 and β-catenin. FN1 is a glycoprotein distributed on the cell surface and in the extracellular matrix, and is involved in endothelium cell invasion, migration and angiogenic processes (15). These processes involve the activation of focal adhesion kinase and the PI3K/AKT/NF-κB signaling pathway (15,23). Previous studies have reported that FN1 is overexpressed in PTC and may serve as a biomarker for PTC diagnosis and treatment (24,25). BSG is a transmembrane protein that is overexpressed in a number of malignant tumor cells, and promotes tumor invasion and metastasis by activating the PI3K/AKT signaling pathway (17,26-29). Previous studies have reported that BSG promotes extra-tumor invasion and lymph metastasis in differentiated thyroid carcinoma (DTC) and is associated with poor prognosis (30,31). PPL, a constituent of desmosomes involved in endothelial cell structure stabilization and considered as a localization signal of AKT, promotes cell growth and survival by binding AKT directly (18). PPL knockdown appeared to decrease the phospho-AKT expression (32,33). Tonoike *et al* (34) demonstrated that PPL knockdown suppresses cell proliferation, migration and invasion through the PI3K/AKT signaling pathway in pharyngeal cancer cells. In the present study, CXCR7 overexpression upregulated the expression of FN1, BSG and PPL, which suggested that CXCR7 may regulate growth and metastasis of PTC via the activation of the PI3K/AKT signaling pathway.

In addition, the results of the present study demonstrated that SERPINB5, a tumor suppressor that belongs to the serpin family, is downregulated following CXCR7 overexpression. SERPINB5 is a tumor protein p53 (p53)-dependent protein that inhibits tumor angiogenesis by interacting with the p53 signaling pathway (21,35). A number of studies have suggested that SERPINB5 inhibits the migration, invasion, metastasis and angiogenesis of tumor cells (22-37). Boltze *et al* (38) and Shams *et al* (39) demonstrated that SERPINB5 is associated with vessel invasion and lymph metastasis in PTC, therefore SERPINB5 can inhibit PTC invasion and metastasis. The results of the present study suggest that CXCR7 promotes PTC growth and metastasis by inhibiting SERPINB5.

The processes of tumor invasion and metastasis include adhesion, degradation and movement (40). The absence of adhesion may induce the degradation of cellular junctions, which is associated with tumor cell invasion and metastasis (41,42). Cellular adhesion comprises cell-cell and cell-matrix contacts, which are distributed in a number of types of tissue, and serve roles in maintaining the integrity of tissues and cells. Adherens junctions are formed by classic cadherins, including epithelial cadherin and neuronal cadherin, which associate with α-/β-catenin, plakoglobin, adherens junction protein p120 and vinculin, and anchor actin microfilaments (43). Calcium-dependent cadherin/catenin/actin cytoskeleton protein complexes serve a vital role in cell morphology maintenance, cell motility and adhesion, cytoskeleton remodeling and regulation of signal transduction (20,44). β-catenin is a multifunctional protein that mediates cell adhesion and signal transduction, and is a component of epithelial cell-cell junctions. However, decreased β-catenin expression and its dysregulation are associated with the initiation of cancer cell invasion and metastasis (20). In the present study, CXCR7 downregulated the expression of β-catenin, which suggests that CXCR7 overexpression may result in the degradation of cellular junctions and the subsequent decrease in cell adhesion, which may eventually lead to the invasion and metastasis of PTC cells.

In addition, the results of the present study identified certain differently expressed proteins with unclear biological

functions, including TAGLN2 and AHNAK2. TAGLN2 is a member of the calponin family of actin-binding proteins and is upregulated in lung cancer, colorectal cancer, and head and neck squamous cell carcinoma (16,45,46). Knockdown of TAGLN2 has been reported to inhibit tumor cell invasion and promote apoptosis (47,48). Notably, it has been reported that the overexpression of TAGLN2 is associated with lymph node metastasis, distant metastasis and tumor-node-metastasis stage in colorectal cancer (47). AHNAK2 is a 600 kDa protein that is expressed in the majority of muscle cells and has a similar function to AHNAK1: It regulates the contraction coupling of myocardial cells through its PSD-95/Discs-large/ZO-1 structural domain (49,50). In addition, AHNAK2 is a constituent of costameres in skeletal muscle and may link the extracellular matrix with the cytoskeleton (19,51). Previous studies have identified that PPL and AHNAK1 affect the formation of the ezrin, PPL, periaxin and desmoyokin skeletal protein complex (52). Therefore PPL, AHNAK2, β-catenin and TAGLN2 are associated with cellular adhesion junctions; overexpression of CXCR7 may lead to dysregulation of these proteins and subsequently degrade cellular junctions, inducing invasion and metastasis of PTC.

In conclusion, the results of the present study provide a possible mechanism for the regulation of PTC invasion and metastasis by CXCR7. Proteomic analysis using iTRAQ-coupled 2D LC-MS/MS identified 130 differentially expressed proteins between GLAG-66 and GLAG-66-CXCR7 cells, including a number of proteins associated with cellular junctions. CXCR7 overexpression may result in the degradation of cellular junctions and therefore promote cell invasion and metastasis. In addition, AHNAK2 and TAGLN2 were identified as potential novel biomarkers for PTC. However, further studies on these proteins are required to demonstrate their function and mechanism in PTC generation and development.

Acknowledgements

The present study was supported by the National Natural Science Foundation of China (grant no. 81072182) and the Natural Science Foundation of Liaoning Province (grant no. 2013021100; China).

References

1. Rahib L, Smith BD, Aizenberg R, Rosenzweig AB, Fleshman JM and Matrisian LM: Projecting cancer incidence and deaths to 2030: The unexpected burden of thyroid, liver, and pancreas cancers in the United States. Cancer Res 74: 2913-2921, 2014.
2. Morris LG, Tuttle RM and Davies L: Changing trends in the incidence of thyroid cancer in the united states. JAMA Otolaryngol Head Neck Surg 142: 709-711, 2016.
3. Podnos YD, Smith D, Wagman LD and Ellenhorn JD: The implication of lymph node metastasis on survival in patients with well-differentiated thyroid cancer. Am Surg 71: 731-734, 2005.
4. Zaydfudim V, Feurer ID, Griffin MR and Phay JE: The impact of lymph node involvement on survival in patients with papillary and follicular thyroid carcinoma. Surgery 144: 1070-1078, 2008.
5. Vandercappellen J, Van Damme J and Struyf S: The role of CXC chemokines and their receptors in cancer. Cancer Lett 267: 226-244, 2008.
6. Ben-Baruch A: Organ selectivity in metastasis: Regulation by chemokines and their receptors. Clin Exp Metastasis 25: 345-356, 2008.
7. Sun X, Cheng G, Hao M, Zheng J, Zhou X, Zhang J, Taichman RS, Pienta KJ and Wang J: CXCL12/CXCR4/CXCR7 chemokine axis and cancer progression. Cancer Metastasis Rev 29: 709-722, 2010.
8. Hao M, Zheng J, Hou K, Wang J, Chen X, Lu X, Bo J, Xu C, Shen K and Wang J: Role of chemokine receptor CXCR7 in bladder cancer progression. Biochem Pharmacol 84: 204-214, 2012.
9. Zheng K, Li HY, Su XL, Wang XY, Tian T, Li F and Ren GS: Chemokine receptor CXCR7 regulates the invasion, angiogenesis and tumor growth of human hepatocellular carcinoma cells. J Exp Clin Cancer Res 29: 31, 2010.
10. Singh RK and Lokeshwar BL: The IL-8-regulated chemokine receptor CXCR7 stimulates EGFR signaling to promote prostate cancer growth. Cancer Res 71: 3268-3277, 2011.
11. Liu Z, Sun DX, Teng XY, Xu WX, Meng XP and Wang BS: Expression of stromal cell derived factor 1 and CXCR7 in papillary thyroid carcinoma. Endocr Pathol 23: 247-253, 2012.
12. Liu Z, Yang L, Teng X, Zhang H and Guan H: The involvement of CXCR7 in modulating the progression of papillary thyroid carcinoma. J Surg Res 191: 379-388, 2014.
13. Zhang H, Teng X, Liu Z, Zhang L and Liu Z: Gene expression profile analyze the molecular mechanism of CXCR7 regulating papillary thyroid carcinoma growth and metastasis. J Exp Clin Cancer Res 34: 16, 2015.
14. Wyllie FS, Lemoine NR, Barton CM, Dawson T, Bond J and Wynford-Thomas D: Direct growth stimulation of normal human epithelial cells by mutant p53. Mol Carcinog 7: 83-88, 1993.
15. Ross PL, Huang YN, Marchese JN, Williamson B, Parker K, Hattan S, Khainovski N, Pillai S, Dey S, Daniels S, *et al*: Multiplexed protein quantitation in Saccharomyces cerevisiae using amine-reactive isobaric tagging reagents. Mol Cell Proteomics 3: 1154-1169, 2004.
16. Paik JY, Ko BH, Jung KH and Lee KH: Fibronectin stimulates endothelial cell 18F-FDG uptake through focal adhesion kinase-mediated phosphatidylinositol 3-kinase/Akt signaling. J Nucl Med 50: 618-624, 2009.
17. Xu XC, Zhang YH, Zhang WB, Li T, Gao H and Wang YH: MicroRNA-133a functions as a tumor suppressor in gastric cancer. J Biol Regul Homeost Agents 28: 615-624, 2014.
18. Fei F, Li X, Xu L, Li D, Zhang Z, Guo X, Yang H, Chen Z and Xing J: CD147-CD98hc complex contributes to poor prognosis of nonsmall cell lung cancer patients through promoting cell proliferation Via the PI3K/Akt signaling pathway. Ann Surg Oncol 21: 4359-4368, 2014.
19. Suzuki A, Horiuchi A, Ashida T, Miyamoto T, Kashima H, Nikaido T, Konishi I and Shiozawa T: Cyclin A2 confers cisplatin resistance to endometrial carcinoma cells via up-regulation of an Akt-binding protein, periplakin. J Cell Mol Med 14: 2305-2317, 2010.
20. de Morrée A, Droog M, Grand Moursel L, Bisschop IJ, Impagliazzo A, Frants RR, Klooster R and van der Maarel SM: Self-regulated alternative splicing at the AHNAK locus. FASEB J 26: 93-103, 2012.
21. Takayama T, Shiozaki H, Shibamoto S, Oka H, Kimura Y, Tamura S, Inoue M, Monden T, Ito F and Monden M: Beta-catenin expression in human cancers. Am J Pathol 148: 39-46, 1996.
22. Zou Z, Anisowicz A, Hendrix MJ, Thor A, Neveu M, Sheng S, Rafidi K, Seftor E and Sager R: Maspin, a serpin with tumor-suppressing activity in human mammary epithelial cells. Science 263: 526-529, 1994.
23. Wang YH, Dong YY, Wang WM, Xie XY, Wang ZM, Chen RX, Chen J, Gao DM, Cui JF and Ren ZG: Vascular endothelial cells facilitated HCC invasion and metastasis through the Akt and NF-κB pathways induced by paracrine cytokines. J Exp Clin Cancer Res 32: 51, 2013.
24. Prasad ML, Huang Y, Pellegata NS, de la Chapelle A and Kloos RT: Hashimoto's thyroiditis with papillary thyroid carcinoma (PTC)-like nuclear alterations express molecular markers of PTC. Histopathology 45: 39-46, 2004.
25. Huang Y, Prasad M, Lemon WJ, Hampel H, Wright FA, Kornacker K, LiVolsi V, Frankel W, Kloos RT, Eng C, *et al*: Gene expression in papillary thyroid carcinoma reveals highly consistent profiles. Proc Natl Acad Sci USA 98: 15044-15049, 2001.
26. Zhang Q, Zhou J, Ku XM, Chen XG, Zhang L, Xu J, Chen GS, Li Q, Qian F, Tian R, *et al*: Expression of CD147 as a significantly unfavorable prognostic factor in hepatocellular carcinoma. Eur J Cancer Prev 16: 196-202, 2007.

27. Wu J, Hao ZW, Zhao YX, Yang XM, Tang H, Zhang X, Song F, Sun XX, Wang B, Nan G, *et al*: Full-length soluble CD147 promotes MMP-2 expression and is a potential serological marker in detection of hepatocellular carcinoma. J Transl Med 12: 190, 2014.
28. Wang L, Wu G, Yu L, Yuan J, Fang F, Zhai Z, Wang F and Wang H: Inhibition of CD147 expression reduces tumor cell invasion in human prostate cancer cell line via RNA interference. Cancer Biol Ther 5: 608-614, 2006.
29. Fang F, Wang L, Zhang S, Fang Q, Hao F, Sun Y, Zhao L, Chen S, Liao H and Wang L: CD147 modulates autophagy through the PI3K/Akt/mTOR pathway in human prostate cancer PC-3 cells. Oncol Lett 9: 1439-1443, 2015.
30. Tan H, Ye K, Wang Z and Tang H: CD147 expression as a significant prognostic factor in differentiated thyroid carcinoma. Transl Res 152: 143-149, 2008.
31. Huang P, Chang S, Jiang X, Su J, Dong C, Liu X, Yuan Z, Zhang Z and Liao H: RNA interference targeting CD147 inhibits the proliferation, invasiveness, and metastatic activity of thyroid carcinoma cells by down-regulating glycolysis. Int J Clin Exp Pathol 8: 309-318, 2015.
32. van den Heuvel AP, de Vries-Smits AM, van Weeren PC, Dijkers PF, de Bruyn KM, Riedl JA and Burgering BM: Binding of protein kinase B to the plakin family member periplakin. J Cell Sci 115: 3957-3966, 2002.
33. Suzuki A, Horiuchi A, Ashida T, Miyamoto T, Kashima H, Nikaido T, Konishi I and Shiozawa T: Cyclin A2 confers cisplatin resistance to endometrial carcinoma cells via up-regulation of an Akt-binding protein, periplakin. J Cell Mol Med 14: 2305-2317, 2010.
34. Tonoike Y, Matsushita K, Tomonaga T, Katada K, Tanaka N, Shimada H, Nakatani Y, Okamoto Y and Nomura F: Adhesion molecule periplakin is involved in cellular movement and attachment in pharyngeal squamous cancer cells. BMC Cell Biol 12: 41, 2011.
35. Zhang M, Volpert O, Shi YH and Bouck N: Maspin is an angiogenesis inhibitor. Nat Med 6: 196-199, 2000.
36. Sheng S, Carey J, Seftor EA, Dias L, Hendrix MJ and Sager R: Maspin acts at the cell membrane to inhibit invasion and motility of mammary and prostatic cancer cells. Proc Natl Acad Sci USA 93: 11669-11674, 1996.
37. Cher ML, Biliran HR Jr, Bhagat S, Meng Y, Che M, Lockett J, Abrams J, Fridman R, Zachareas M and Sheng S: Maspin expression inhibits osteolysis, tumor growth, and angiogenesis in a model of prostate cancer bone metastasis. Proc Natl Acad Sci USA 100: 7847-7852, 2003.
38. Boltze C, Schneider-Stock R, Meyer F, Peters B, Quednow C, Hoang-Vu C and Roessner A: Maspin in thyroid cancer: Its relationship with p53 and clinical outcome. Oncol Rep 10: 1783-1787, 2003.
39. Shams TM, Samaka RM and Shams ME: Maspin protein expression: A special feature of papillary thyroid carcinoma. J Egypt Natl Canc Inst 18: 274-280, 2006.
40. Liotta LA and Stetler-Stevenson WG: Tumor invasion and metastasis: An imbalance of positive and negative regulation. Cancer Res 51 (18 Suppl): 5054s-5059s, 1991.
41. Kleinberg L, Holth A, Fridman E, Schwartz I, Shih IeM and Davidson B: The diagnostic role of claudins in serous effusions. Am J Clin Pathol 127: 928-937, 2007.
42. Ohtani S, Terashima M, Satoh J, Soeta N, Saze Z, Kashimura S, Ohsuka F, Hoshino Y, Kogure M and Gotoh M: Expression of tight-junction-associated proteins in human gastric cancer: Downregulation of claudin-4 correlates with tumor aggressiveness and survival. Gastric Cancer 12: 43-51, 2009.
43. Huber O, Bierkamp C and Kemler R: Cadherins and catenins in development. Curr Opin Cell Biol 8: 685-691, 1996.
44. Miller JR and Moon RT: Signal transduction through beta-catenin and specification of cell fate during embryogenesis. Genes Dev 10: 2527-2539, 1996.
45. Rho JH, Roehrl MH and Wang JY: Tissue proteomics reveals differential and compartment-specific expression of the homologs transgelin and transgelin-2 in lung adenocarcinoma and its stroma. J Proteome Res 8: 5610-5618, 2009.
46. Zhang Y, Ye Y, Shen D, Jiang K, Zhang H, Sun W, Zhang J, Xu F, Cui Z and Wang S: Identification of transgelin-2 as a biomarker of colorectal cancer by laser capture microdissection and quantitative proteome analysis. Cancer Sci 101: 523-529, 2010.
47. Nohata N, Sone Y, Hanazawa T, Fuse M, Kikkawa N, Yoshino H, Chiyomaru T, Kawakami K, Enokida H, Nakagawa M, *et al*: miR-1 as a tumor suppressive microRNA targeting TAGLN2 in head and neck squamous cell carcinoma. Oncotarget 2: 29-42, 2011.
48. Li AY, Yang Q and Yang K: miR-133a mediates the hypoxia-induced apoptosis by inhibiting TAGLN2 expression in cardiac myocytes. Mol Cell Biochem 400: 173-181, 2015.
49. Shtivelman E, Cohen FE and Bishop JM: A human gene (AHNAK) encoding an unusually large protein with a 1.2-microns polyionic rod structure. Proc Natl Acad Sci USA 89: 5472-5476, 1992.
50. Komuro A, Masuda Y, Kobayashi K, Babbitt R, Gunel M, Flavell RA and Marchesi VT: The AHNAKs are a class of giant propeller-like proteins that associate with calcium channel proteins of cardiomyocytes and other cells. Proc Natl Acad Sci USA 101: 4053-4058, 2004.
51. Marg A, Haase H, Neumann T, Kouno M and Morano I: AHNAK1 and AHNAK2 are costameric proteins: AHNAK1 affects transverse skeletal muscle fiber stiffness. Biochem Biophys Res Commun 401: 143-158, 2010.
52. Straub BK, Boda J, Kuhn C, Schnoelzer M, Korf U, Kempf T, Spring H, Hatzfeld M and Franke WW: A novel cell-cell junction system: The cortex adherens mosaic of lens fiber cells. J Cell Sci 116: 4985-4995, 2003.